

Insights on Interfacial Charge Transfer Across P3HT/Fullerene Photovoltaic Heterojunction from Ab Initio Calculations

Yosuke Kanai* and Jeffrey C. Grossman*

Berkeley Nanosciences and Nanoengineering Institute and Center of Integrated Nanomechanical Systems, University of California, Berkeley, California 94720

Received March 26, 2007; Revised Manuscript Received May 11, 2007

ABSTRACT

The interfacial charge-transfer mechanism of the P3HT/fullerene photovoltaic heterojunction is elucidated using density functional theory calculations. Our findings indicate that an efficient adiabatic electron transfer is highly probable due to the presence of an extended electronic state that has a significant probability distribution across the interface in the lowest excited state. Furthermore, efficient exciton dissociation is possible because this bridging state has significant overlap with near-degenerate unoccupied states that are localized on the fullerene.

Recent advances make nanomaterials ideal for photovoltaic (PV) applications^{1–3} because of the ability to engineer and tailor their optical and electronic properties by controlling the material size, shape, and surface while maintaining low cost. One promising class of nanoPV devices is the excitonic solar cell (XSC),⁴ although the experimental realization of efficient PV devices based on the XSC concept remains highly challenging. Compared with conventional cells, excitons are more strongly bound in XSCs and must be dissociated at an interface of two different materials in order to produce charge carriers.⁵ Therefore, the electronic properties of this nanoscale interface are of fundamental importance for the production of free charge carriers and essential for efficient XCS devices.

One of the most successful XSCs is based on a polymer/fullerene blend.² In particular, a ~5% power conversion efficiency reported⁶ for the poly-3-hexylthiophene (P3HT)/fullerene device is quite encouraging, especially given that the P3HT phase absorbs only about 20% of standard AM1.5 solar photons due to the spectral mismatch⁷ (relaxation of the photoexcited electron further reduces the maximum attainable efficiency). While there could be a number of physical processes limiting the efficiency, the charge separation process in this PV cell is known to be extremely efficient, leading to an external quantum efficiency over 70%.⁸ Thus, understanding the mechanism of the charge separation process in this particular cell may have broad implications for XSC designs in general. Charge separation

at the heterojunction interface involves the dissociation of an exciton that has diffused from within the polymer to the interface, transferring the electron to the fullerene side while leaving the hole behind in the polymer phase. An ultrafast (subpicosecond) interfacial electron transfer is known to be operative in these types of interfaces based on photoinduced absorption and light-induced electron spin resonance experiments for some π -conjugated polymers.^{9–13} While this fast electron transfer is clearly beneficial for promoting an efficient charge separation process in the PV cell, its mechanism for the polymer/fullerene heterojunction is at present not well understood and remains little explored theoretically at an atomistic level.¹⁴

In another type of PV device, the dye-sensitized solar cell (DSSC),¹⁵ a conventional nonadiabatic electron-transfer mechanism can successfully explain the observed ultrafast charge transfer. By invoking Fermi's golden rule with semi-infinite acceptor (final) states in the conduction band (CB) of TiO₂, the photoexcited electron within the dye has a very high total transition probability to the TiO₂.¹⁶ In recent years, ab initio studies have been used to explore charge-transfer mechanisms with different chromophores for DSSC.¹⁷ For example, using a nonadiabatic molecular dynamics simulation approach,¹⁸ Duncan et al. showed that an alternative adiabatic mechanism is dominant with the Alizarin chromophore, for which the photoexcited state lies at the edge of TiO₂ CB minimum.¹⁹

The ultrafast electron transfer for the polymer/fullerene heterojunction interface is also difficult to reconcile in the standard nonadiabatic picture because the density of final

* E-mail: ykanai@berkeley.edu (Y.K.); jgrossman@berkeley.edu (J.C.G.).

states (of the electron transfer) is rather limited, unlike in the CB of TiO₂. It is therefore reasonable to suspect that other electron-transfer mechanisms are operative in this case as well.

Experimental exploration into the local electronic structure of the heterojunction interface poses enormous challenges, although recently the molecular structure of the interface was probed by Yang et al. using NMR,²⁰ showing a clear structural separation of the two phases at an atomistic level for the annealed interface. From a theoretical standpoint, understanding the nature of charge separation at the interface inherently requires an accurate quantum mechanical description of its structural and electronic properties.

In this letter, the electronic structure of the P3HT/C₆₀ heterojunction interface is probed using ab initio density functional theory (DFT) calculations in order to gain insight into the interfacial charge-transfer mechanism. Our findings indicate that a very efficient *adiabatic* electron transfer from P3HT to the fullerenes is highly probable. There exists an extended electronic state (for the excited transferring electron) that has a significant probability distribution *across* the interface in the lowest excited state, which is energetically favorable even for the thermally relaxed exciton diffusing through the P3HT phase. Indeed, this bridging electronic state is formed by “hybridizing” a P3HT π^* state with a triply degenerate unoccupied state of the fullerene. Furthermore, this bridging electronic state has a significant overlap with other unoccupied fullerene states that are energetically very close (~ 0.01 eV), deriving exclusively from the triply degenerate t_{1u} states of the fullerene. Exciton dissociation can therefore efficiently follow to form bound-ion pairs by coupling to the fullerene-localized states via vibronic interactions due to their near degeneracy to the bridging state. These two physical attributes in combination provide an important route for an efficient charge separation process in XSC heterojunctions.

The electronic and structural properties of the systems considered in this work were obtained using DFT, employing a nonempirical gradient-corrected exchange-correlation functional.²¹ Ultrasoft pseudopotentials²² are used to describe the core electrons, and the wave functions and charge density are expanded in plane waves with kinetic energy up to 25 and 160 Ry, respectively. We used an orthorhombic simulation cell with periodic boundary conditions of dimensions 26.46/26.46/15.72 ($x/y/z$) Å, in which a regioregular P3HT polymer chain lies in the z direction. The simulation cell contains four thiophene units of the polymer in the z direction, separated by vacuum regions in the other two directions to prevent chain–chain interactions (see Figure 1).

A single thiophene unit length of P3HT is calculated to be 3.93 Å, in good agreement with the experimental value of around 3.9 Å.²³ The highest occupied molecular orbital (HOMO) and lowest unoccupied molecular orbital (LUMO) are π and π^* in character, respectively. The calculated HOMO–LUMO gap of 1.15 eV from the Kohn–Sham (KS) single-particle states is substantially lower than the experimental band gap (~ 1.9 eV), as is generally observed in the

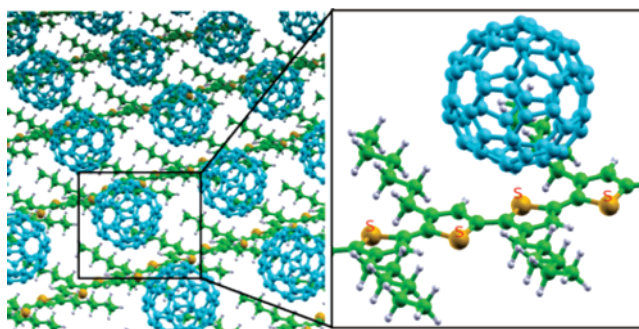


Figure 1. Model interface used in the calculations. The box indicates a periodically repeated simulation cell that contains a C₆₀ molecule and four thiophene units of a P3HT polymer.

DFT–KS approach. The π (π^*) state is energetically well separated from the lower occupied (higher unoccupied) states. Introducing another P3HT chain parallel to the original one reduces the gap by less than 0.1 eV in our calculations.

The icosahedral symmetry (I_h) of the C₆₀ molecule leads to a set of highly degenerate electronic states with a triply degenerate LUMO. The underestimation of the computed DFT–KS gap (1.64 eV) should be noted again, compared to the experimental gap of around 2.6 eV.²⁴ The exceptionally high electron affinity (EA) of the C₆₀ molecule is quite important for charge transfer and is well described in our calculations. The vertical (adiabatic) EA is determined to be 2.70 (2.75) eV, in excellent agreement with the experimental value of 2.69 eV,²⁵ as also reported earlier using DFT.²⁶

The heterojunction interface is modeled using a single C₆₀ molecule per unit cell as shown in Figure 1. In this case, the interaction between adjacent C₆₀ molecules is negligible, and the polymer/fullerene mass ratio is 1:1.1, close to the mass percentage ratio of 50:50 often used in experiments, although the exact ratio at the interface is unknown. We note that the results of our calculations should not depend strongly on this ratio because even a modest doping of P3HT with C₆₀ molecules is enough to observe the ultrafast photoinduced charge transfer,²⁷ and furthermore, the dependence on this ratio at the interface is discussed later in the text and found to be negligible.

Structural optimization starting from C₆₀ placed along the polymer chain led to two energy minima with the C₆₀ molecule interacting directly with a thiophene ring, contacting through two different nonequivalent C₆₀ faces. This geometrical orientation found in our calculation is consistent with a recent experimental NMR study of the interaction of C₆₀ with the thiophene ring.²⁰ The interaction energy of C₆₀ and P3HT was calculated to be 0.06 eV for the pentagon of C₆₀ facing a thiophene ring, 0.02 eV larger than for the case with the hexagon facing the thiophene ring. The distance between C₆₀ and P3HT is on the order of 3.5 Å in the perpendicular direction to the polymer chain for both cases. Regardless of which face is interacting, the maximum deviation for carbon atoms in terms of the radial distance from the center (3.56 Å in the isolated C₆₀) was calculated to be only about +0.01 Å. As expected, the carbon atoms with the most distortion are those constituting the interacting

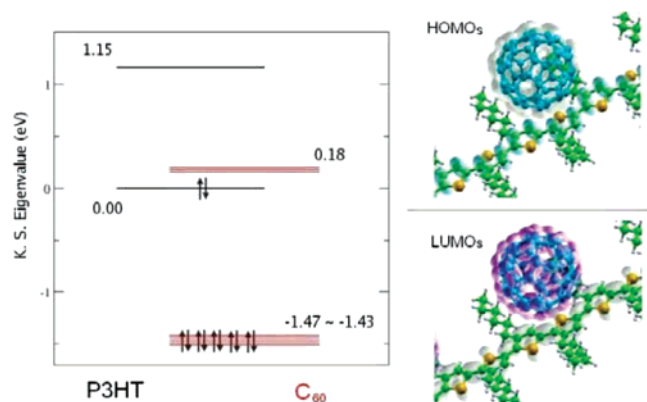


Figure 2. KS single-particle states of the combined C_{60} /P3HT system. The isosurface of each state is plotted at 0.001 au. The highest (blue) and next-highest (gray) occupied states are of HOMOs of P3HT and C_{60} in character, respectively (upper right). The lowest (red) and next-lowest (gray) unoccupied states are of LUMOs of C_{60} and P3HT in character, respectively (lower right). Energy levels are shown (left) and shifted in the horizontal direction to indicate whether corresponding states are localized on P3HT (left) or C_{60} (right). The eigenvalue of the P3HT π state is taken as the reference energy (0 eV).

pentagon or hexagon faces. Such a distortion of the potential energy surface for C_{60} could be the source of the splitting in the ^{13}C NMR chemical shift peaks observed in ref 20. The slightly more stable case of the pentagon facing the polymer chain will be considered henceforth.

The charge transfer between C_{60} and P3HT is quantified by projecting the electron density onto that of orthogonalized atomic wave functions, which unambiguously belong to either of the two systems. Taking the difference between the projection on the interacting and individual P3HT/ C_{60} systems, we found very little charge transfer ($\sim 0.1 e$) from P3HT to C_{60} in the electronic ground state. Although there is some experimental evidence that charge transfer is possible even in the ground state,²⁸ such a small computed value indicates that this charge transfer is not efficient and highly unlikely to be responsible for charge separation at the heterojunction. The single-particle states and corresponding energy levels in the vicinity of the Fermi level for this interface are shown in Figure 2; a clear spatial separation of the P3HT and C_{60} single-particle states were observed. As can be seen, the offsets of the HOMO and LUMO levels for the two interacting systems are those of a type-II heterojunction. From the energy level alignment and spatial separation of the LUMOs in the ground state, one might anticipate a rather inefficient excited electron transfer through these states. However, the nanoscale P3HT/ C_{60} heterojunction is locally molecular in nature (unlike a macroscopic heterojunction interface in many solid-state systems), thus the understanding of its excited-state properties is rather limited from a ground state picture. More specifically, for this particular interface, the transfer of the excited electron to C_{60} within such a confined space would certainly change the electrostatic potential in the nearby vicinity and therefore the alignment of energy levels at the interface.

Solar photons dominantly excite P3HT via the $\pi \rightarrow \pi^*$ transition. Given that a majority of the excitons are formed

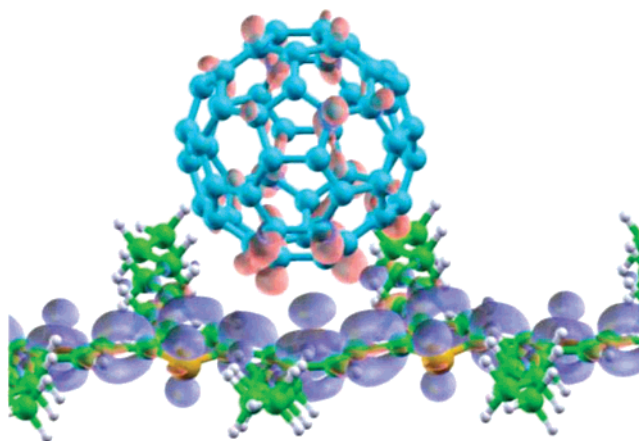


Figure 3. Addition (red) and depletion (blue) regions of electron charge density in the lowest excited state with respect to the noninteracting systems of P3HT in the triplet excited state and the ground-state C_{60} . The isosurfaces are plotted at ± 0.001 au.

in the bulk polymer phase and diffuse before reaching the interface, excitons dissociating at the heterojunction are mostly in the lowest excited state in P3HT (π^* state). Within the conventional acceptor–donor XSC framework, this excited electron transfers to the t_{1u} LUMO state of C_{60} . Whether the singlet or triplet manifold is dominant is expected to depend strongly on the effective conjugation length and regioregularity of P3HT, although the intersystem crossing to triplet is rather efficient for polythiophenes and triplet excitons have a much longer lifetime.²⁹ We discuss here only the triplet case because our calculations show that the same conclusions can be drawn for the singlet manifold (see Supporting Information). For those photoexcited electrons formed *directly* at the interface, the charge-transfer mechanism can in principle vary depending on the absorbing photon wavelength.

The lowest excited states of the spin triplet manifold are determined to lie 0.76 eV above the ground state (the singlet state is an additional 0.12 eV higher).³⁰ For the lowest triplet excited state at the ground-state geometry, our calculations show a significant charge transfer from P3HT to C_{60} —approximately $0.55 e$ is transferred to the fullerene atoms. Changes in the electronic charge density of the interface with respect to the noninteracting systems of P3HT in the triplet excited state and the ground-state C_{60} are shown in Figure 3. A depletion of density from the π^* state of P3HT is evident, and the charge increase on C_{60} is not localized near the contacting atoms, indicating that the charge transfer is mainly nonelectrostatic in nature. More importantly, *partial* transfer of an electron was observed despite the fact that the electrostatic interaction is not responsible for the charge transfer. The formation of such an asymmetric “exciplex” at the interface has been documented previously experimentally for a system of conjugated polymers and fullerenes in a nonpolar solution.³¹

To understand the nature of this charge-transfer further, we analyzed select single-particle states occupied by the transferring excited electron. The spatial extents of these states and energies of the states nearby are shown in Figures 4 and 5, respectively. The transferring electron is found to

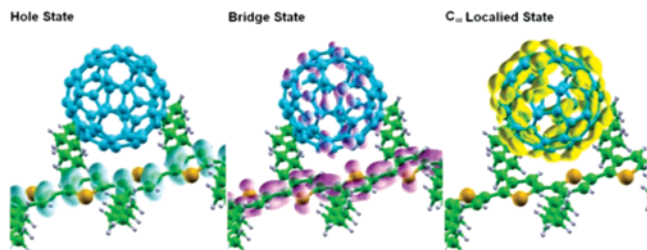


Figure 4. Isosurface of the hole state, bridging state where the excited electron occupies, and the near-degenerate C_{60} -localized state for the P3HT/ C_{60} interface (plotted at 0.001 au). See also Figure 5.

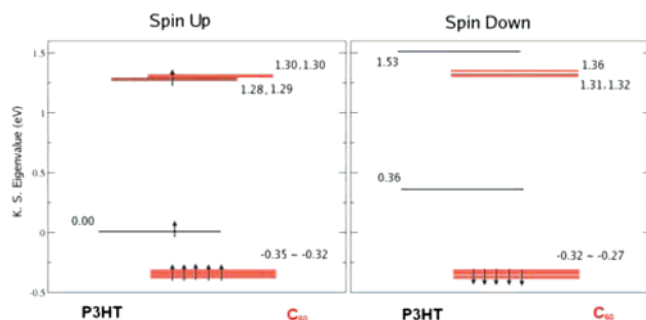


Figure 5. KS single-particle states of the P3HT/ C_{60} interface close to the Fermi level in the lowest excited state. Energy levels are shifted in the horizontal direction to indicate whether the corresponding states are localized on P3HT (left) or C_{60} (right). The eigenvalue of the singly occupied P3HT π state is taken as the reference energy (0 eV).

occupy a highly extended single-particle state whose probability distribution bridges the P3HT and C_{60} , while the unoccupied hole remains as the P3HT π state. The projection analysis of this single extended bridging state, occupied by the transferring charge, reveals that 52% and 48% of the probability density situate on C_{60} and P3HT, respectively. These single-particle states in the immediate vicinity of the bridge state derive from the P3HT π^* LUMO state and triply degenerate t_{1u} LUMO states of C_{60} . In this lowest excited state, the π^* state and one of the t_{1u} states “hybridize” to form a pair of bridging states, one of which is occupied by the excited electron. The other two states deriving from the C_{60} t_{1u} states are highly localized on the fullerene and are essentially degenerate (within 0.01 eV) with the bridging states. Although the π^* and t_{1u} states are quite separated energetically in the ground state, the electrostatic potential across the P3HT/ C_{60} interface changes significantly due to the charge transfer in the excited state, which in turn causes the eigenvalues to become close in energy. Such a change in energetic alignment of the states can be readily observed in the case of the down-spin orbitals for which these single-particle states are unoccupied (Figure 5).

Regarding the interfacial charge-transfer mechanism, our results indicate that an efficient electron transfer is highly probable due to the strong overlap of wave functions between the excited P3HT and the fullerene. The electron transfers adiabatically by occupying the bridging state in the lowest excited-state once the exciton diffuses to the interface region, which can explain the experimental observation^{9–13} of

ultrafast charge transfer. Of fundamental importance for the charge separation process are the closely lying single-particle states just above (energetically) this electron-transferring bridge state, as they can facilitate the exciton dissociation (complete transfer) to form the bound ion pairs. Large vibronic couplings are expected among them because of the near degeneracy of these single-particle states and significant spatial overlap with the bridge state. Indeed, thermal averaging of the near-degenerate t_{1u} states in the C_{60} anion is well-documented experimentally.^{27,32,33} The near-degenerate single-particle states enable efficient exciton dissociation and reduce the probability of the electron to recombine with the hole through the bridge state.

Another possible mechanism for exciton dissociation is the level-reordering of the near-degenerate single-particle states, induced by geometrical changes. For the C_{60} anion, it is well-known that geometrical distortions are strongly coupled to the electronic structure and, particularly, the t_{1u} state is split into a combination of singly and doubly degenerate states.³³ To address this possibility, we studied how a geometric relaxation in the lowest excited state might influence the ordering of those near-degenerate energy levels. We computed a rather large Stokes shift of 0.33 eV and found that the C_{60} molecule shifts away from the polymer by ~ 0.15 Å. The maximum radial distortion of C_{60} was $+0.007$ Å for the atoms contained in the pentagon facing the polymer. At this relaxed geometry, we still observed the partial charge transfer of approximately $0.45 e$ to the fullerene, together with the same qualitative features of the single-particle states. The energy splitting of the occupied bridging state and unoccupied one slightly increased to 0.02 eV, and the other two C_{60} -localized states were also pushed up in energy by 0.03 eV. In addition, a short first-principles molecular dynamics simulation was carried out to assess how the relaxation energy might lead to large distortions of the fullerene through an increase in the kinetic energy. We observed a maximum spherical distortion of the fullerene of only ~ 0.015 Å, and level-reordering among these near-degenerate single-particle states was *not* observed (see Supporting Information). This implies that a geometrical-induced (Stokes shift) level-reordering is unlikely to play a dominant role in exciton dissociation.

The dependence of our results on the P3HT polymer structure at the interface was investigated in order to gain insight on how the charge separation process is affected by its variation. In particular, four structural variations were considered (see Figure 6): (A) a larger P3HT/fullerene ratio, (B) addition of a second polymer layer, (C) interdigitized alkyl chains with adjacent polymers, and (D) a highly strained polymer. We addressed effects of the fullerene/polymer ratio by increasing the number of thiophene units per fullerene from four to six in the simulation cell in case (A). For case (B), a second layer of polymer was placed directly beneath the first layer and the interchain distance was calculated to be 4.0 Å (in good agreement with the corresponding experimental value of 3.8 Å).³⁴ For case (C), the simulation cell in the alkyl chain direction was reduced to 16.2 Å as in crystalline P3HT,²⁰ such that the alkyl chains

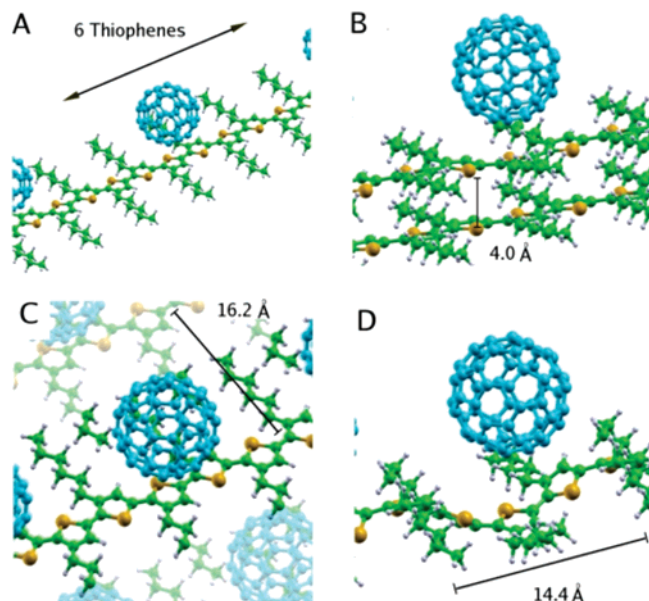


Figure 6. Four variations of the P3HT/ C_{60} interface, used to assess the structural dependence. (A) larger P3HT/fullerene ratio, (B) addition of a second polymer layer, (C) interdigitized alkyl chains with adjacent polymers, and (D) highly strained polymer.

Table 1. Comparison of Several Key Electronic Structure Properties for the Four Different Structural Variations as in Figure 6^a

	regular	A	B	C	D
CT (e)	0.55	0.55	0.59	0.48	0.57
state (%)	52	54	53	42	49
brid (eV)	0.01	0.00	0.00	0.01	0.02
locA (eV)	0.02	0.01	0.02	0.02	0.02
locB (eV)	0.02	0.02	0.02	0.02	0.01
hole (eV)	−0.92	−0.93	−0.83	−1.26	−1.17
TE (eV)	0.76	0.73	0.60	0.77	0.92

^a CT: The extent of charge transfer to the fullerene. State: percentage of the bridge state on the fullerene. Brid, LocA, LocB: energies of the unoccupied bridge and two fullerene-localized single-particle states with respect to the occupied bridge single-particle state, respectively. Hole: energy of the hole state with respect to the occupied bridge single-particle state. TE: the total energy of the system in the lowest excited state with respect to the ground state.

of adjacent polymers are interacting strongly. For case (D), we assessed the effects of P3HT nonplanarity by inducing a significant strain (0.2 eV per thiophene unit) via 8.3% reduction of the simulation cell in the chain direction. In all cases, our calculations show qualitatively the same amount of partial charge transfer in the lowest excited state of half an electron to the fullerene as well as the energy alignment, as summarized in Table 1. These results suggest that the partial charge transfer and exciton dissociation steps do not depend greatly on the local structural details of P3HT. Rather, it can be inferred that the observed increase in the power conversion efficiency upon annealing is due to other important attributes such as separation from the bound ion pairs into free charge carriers and charge mobility.

Chemical functionalization of the C_{60} molecule (as in the case of [6,6]-phenyl- C_{61} butyric acid methyl ester (PCBM)) is another key parameter affecting the charge separation

process because the triply degenerate t_{1u} LUMO states of C_{60} are important for exciton dissociation in the above-mentioned mechanism. Covalent functionalization in general could change the relevant energetics by inducing a splitting of the degenerate LUMO states. In the case of PCBM, the covalently bonded side chain at the [6,6] position, however, breaks the degeneracy of the LUMO and HOMO only marginally. In the lowest excited state, we found 0.51 e transferred to PCBM, similar to the case of C_{60} . Single-particle states near the Fermi level are found to have essentially the same features as for the case of C_{60} , except that one of the unoccupied PCBM-localized states is approximately 0.2 eV higher in energy than the bridging state (see Supporting Information). Therefore, PCBM may possess somewhat less efficient exciton dissociation compared to C_{60} due to the reduced degeneracy of the fullerene-localized states.

In conclusion, a first-principles DFT approach is employed to elucidate the mechanism responsible for charge separation at the P3HT/fullerene heterojunction. We showed that the electronic structure of the lowest excited state is significantly different from what might be expected from the ground-state picture, effectively due to the molecular nature of the heterojunction interface. More specifically, the energy alignment of electronic single-particle states at the interface is significantly altered in the excited-state because of the transferring charge (via an inductive change in the potential across the interface) in this nanoscale heterojunction. We found that there is a significant overlap between the wave functions of P3HT and C_{60} in the lowest excited state, in the form of an extended excited electron state bridging the two, even though the LUMOs of each system have insignificant overlap with each other in the ground state. Such a strong overlap of wave functions in the excited state has been proposed previously to account for the observed ultrafast charge transfer.^{9,35} This excited state is of exciplex in nature with a large asymmetric character for the excited electron and hole; Lin, et al. have previously reported this asymmetry experimentally for a system of conjugated polymer and fullerene.³¹ Our results indicate that the electron transfer in the P3HT/fullerene heterojunction is likely to be an adiabatic transfer in the lowest excited state, where an extended single-particle state bridges across the interface for the excited electron. There exist also near-degenerate unoccupied single-particle states (deriving from fullerene LUMO states) immediately above the electron-transferring bridging state. We suggest that such a near degeneracy enables this asymmetric exciplex state to act as an effective *intermediate* state for transferring the charge to facilitate the exciton dissociation (complete transfer). We therefore expect that the disruption of the fullerene's degenerate LUMO states in general could lead to a less efficient exciton dissociation. Covalent functionalization of fullerenes is in general prone to such a disruption of the LUMO degeneracy, although we found the disruption to be minor in the case of PCBM.

In addition to the important *energetic* criteria of Type-II offsets for HOMOs and LUMOs for favorable charge separation, fast charge transfer is another important *kinetic*

criterion for the process because of other competing mechanisms such as the exciton recombination within the donor phase. We suggest that the strong wave function overlap in the excited state partly satisfies this important criterion and allows for a fast adiabatic electron transfer. The existence of such an adiabatic transfer channel alone, however, may not necessarily lead to an efficient charge separation process unless there exist in the energetic vicinity other states that can facilitate the exciton dissociation efficiently, as observed in the P3HT/fullerene interface.

The results presented here suggest that a XSC design satisfying the above-mentioned kinetic criterion may be more easily achieved with solid-state structures where the conduction band (CB) could offer a large density of "escape channel" states for the transferring electron to enable efficient exciton dissociation. By engineering, for example, the molecular chemistry at the surface, one can also envision tailoring the electronic structure such that the bridging state for the transferring electron forms near the CB minimum. Use of carbon nanotubes in place of fullerenes as done in recent experiments³⁶ is another interesting avenue in this regard.

Acknowledgment. We thank D. Okawa, B. Kessler, and K. Sivula for useful discussions. This work was performed under the auspices of the National Science Foundation by University of California Berkeley under grant no. 0425914, and by funding from the Industrial Technology Research Institute. Computations were performed at the National Energy Research Scientific Computing Center. The Quantum-Espresso code (www.quantum-espresso.org) was used for calculations.

Supporting Information Available: Figures for density of states of P3HT and the fullerenes, single-particles energy levels in the lowest singlet excited state, and the results for the case of PCBM. Computational details of the first-principles molecular dynamics simulation. This material is available free of charge via the Internet at <http://pubs.acs.org>.

References

- (1) Huynh, W.; Dittmer, J. J.; Alivisatos, A. P. *Science* **2002**, 295, 2425.
- (2) Brabec, C. J.; Sariciftci, N. S.; Hummelen, J. C. *Adv. Funct. Mater.* **2001**, 11, 15.
- (3) Coakley, K. M.; Liu, Y.; Chiatzun, G.; McGehee, M. D. *MRS Bull.* **2005**, 30, 37.
- (4) Forrest, S. R. *MRS Bull.* **2005**, 30, 28.
- (5) Gledhill, S. E.; Scott, B.; Gregg, B. A. *J. Mater. Res.* **2005**, 20, 3167.
- (6) Ma, W.; Yang, C.; Gong, X.; Lee, K.; Heeger, A. J. *Adv. Funct. Mater.* **2005**, 15, 1617.
- (7) Coakley, K. M.; McGehee, M. D. *Chem. Mater.* **2004**, 16, 4533.
- (8) Padinger, F.; Rittberger, R. S.; Sariciftci, N. S. *Adv. Funct. Mater.* **2003**, 13, 85.
- (9) Sariciftci, N. S.; Smilowitz, L.; Heeger, A. J.; Wudl, F. *Science* **1992**, 258, 1474.
- (10) Kraabel, B.; Hummelen, J. C.; Vacar, D.; Moses, D.; Sariciftci, N. S.; Heeger, A. J.; Wudl, F. *J. Chem. Phys.* **1996**, 104, 4268.
- (11) Brabec, C. J.; Zerza, G.; Cerullo, G.; De Silvestri, S.; Luzzati, S.; Hummelen, J. C.; Sariciftci, N. S. *Chem. Phys. Lett.* **2001**, 340, 232.
- (12) Kraabel, B.; McBranch, D.; Sariciftci, N. S.; Moses, D.; Heeger, A. J. *Phys. Rev. B* **1994**, 50, 18543.
- (13) Ai, X.; Beard, C. M.; Knutsen, K. P.; Shaheen, S. E.; Rumbles, G.; Ellingson, R. J. *J. Phys. Chem. B* **2006**, 110, 25462.
- (14) Liu, Y.-X.; Summers, M. A.; Scully, S. R.; McGehee, M. D. *J. Appl. Phys.* **2006**, 99, 093521.
- (15) Gratzel, M. *Inorg. Chem.* **2005**, 44, 6841.
- (16) Durrant, J. R.; Haque, S. A.; Palomares, E. *Chem. Commun.* **2006**, 31, 3279.
- (17) For a recent review, see, e.g., Duncan, W. R.; Prezhd, O. V. *Annu. Rev. Phys. Chem.* **2007**, 58, 143.
- (18) Craig, C. F.; Duncan, W. R.; Prezhd, O. V. *Phys. Rev. Lett.* **2005**, 95, 163001.
- (19) Duncan, W. R.; Stier, W. M.; Prezhd, O. V. *J. Am. Chem. Soc.* **2005**, 127, 7941.
- (20) Yang, C.; Hu, J. G.; Heeger, A. J. *J. Am. Chem. Soc.* **2006**, 128, 12007.
- (21) Perdew, J.; Burke, K.; Ernzerhof, M. *Phys. Rev. Lett.* **1996**, 77, 3865.
- (22) Vanderbilt, D. *Phys. Rev. B* **1990**, 41, 7892.
- (23) Prosa, T. J.; Winokur, M. J.; Moulton, J.; Smith, P.; Heeger, A. J. *Macromolecule* **1992**, 25, 4364.
- (24) Hebard, A. F. *Annu. Rev. Mater. Sci.* **1993**, 23, 159.
- (25) Wang, X.-B.; Ding, C.-F.; Wang, L.-S. *J. Chem. Phys.* **1999**, 110, 8217.
- (26) Andreoni, W. *Annu. Rev. Phys. Chem.* **1998**, 49, 405.
- (27) Marumoto, K.; Takeuchi, N.; Ozaki, T.; Kuroda, S. *Synth. Met.* **2002**, 129, 239.
- (28) Morita, S.; Zakhidov, A. A.; Yoshino, K. *Solid State Commun.* **1992**, 82, 2084.
- (29) (a) Jiang, X. M.; Österbacka, R.; Korovyanko, O.; An, C. P.; Horowitz, B.; Janssens, R. A.; Vardeny, Z. V. *Adv. Funct. Mater.* **2002**, 12, 593. (b) Kraabel, B.; Moses, D.; Heeger, A. J. *J. Chem. Phys.* **1995**, 103, 5102. (c) Rentsch, S.; Yang, J. P.; Paa, W.; Birkner, E.; Schiedt, J. Weinkauff *Phys. Chem. Chem. Phys.* **1999**, 1, 1707. (d) Janssens, R. A.; Smilowitz, L.; Sariciftci, N. S.; Moses, D. *J. Chem. Phys.* **1994**, 101, 1788.
- (30) The lowest excited state of the triplet manifold was obtained using spin-polarized calculation by constraining the spin symmetry $S_z = 1$. We determined the singlet excited state energy by using Δ SCF approach. Ziegler, T. *Chem. Rev.* **1991**, 91, 651.
- (31) Lin, H.; Weng, Y.; Huang, H.; He, Q.; Zheng, M.; Bai, F. *Appl. Phys. Lett.* **2004**, 84, 2980.
- (32) Dyakonov, V.; Zorinians, G.; Scharber, M.; Brabec, C. J.; Janssens, R. A.; Hummelen, J. C.; Sariciftci, N. S. *Phys. Rev. B* **1999**, 59, 8019.
- (33) Stinchcombe, J.; Pénicaud, A.; Bhyrappa, P.; Boyd, P. D. W.; Reed, C. A. *J. Am. Chem. Soc.* **1993**, 115, 5212.
- (34) Ma, W.; Yang, C.; Gong, X.; Lee, K.; Heeger, A. J. *Adv. Funct. Mater.* **2005**, 15, 1617.
- (35) Koepp, R.; Sariciftci, N. S. *Photochem. Photobiol. Sci.* **2006**, 5, 1122.
- (36) Kymakis, E.; Amaratunga, G. A. J. *Rev. Adv. Mater. Sci.* **2005**, 10, 300.

NL0707095